

Non-Gaussianity from Features

S. Basu^{1*}, D. J. Brooker^{2*}, N. C. Tsamis^{3†} and R. P. Woodard^{1‡}

¹ *Department of Physics, University of Florida,
Gainesville, FL 32611, UNITED STATES*

² *U.S. Naval Research Laboratory, Code 7160,
4555 Overlook Ave., SW, Washington, DC 20375, UNITED STATES*

³ *Institute of Theoretical Physics & Computational Physics,
Department of Physics, University of Crete,
GR-710 03 Heraklion, HELLAS*

ABSTRACT

The strongest non-Gaussianity in single-scalar potential models of inflation is associated with features in the power spectrum. We stress the importance of accurately modelling the expected signal in order for the standard estimator to minimize contamination by random noise. We present explicit formulae which improve on the approximation introduced by Adshead, Hu, Dvorkin and Peiris. We also use Planck data to compute the non-Gaussian signal, and its error, from a simplified model of the first feature. Our result is $\mathcal{E} = 0.36 \pm 196$.

PACS numbers: 04.50.Kd, 95.35.+d, 98.62.-g

* e-mail: shinjinibas@ufl.edu

* e-mail: daniel.brooker@nrl.navy.mil

† e-mail: tsamis@physics.uoc.gr

‡ e-mail: woodard@phys.ufl.edu

1 Introduction

The prediction of primordial scalar perturbations [1] in single-scalar inflation described by the Lagrangian,

$$\mathcal{L} = \frac{R\sqrt{-g}}{16\pi G} - \frac{1}{2}\partial_\mu\varphi\partial_\nu\varphi g^{\mu\nu}\sqrt{-g} - V(\varphi)\sqrt{-g}. \quad (1)$$

represents the first (and so far only) observed quantum gravitational phenomena [2–4]. It is frustrating that we do not know the scalar potential $V(\varphi)$, or even if single-scalar inflation is correct. It is also frustrating that so little guidance for fundamental theory is provided by observation. The approximately 10^7 pixels of data from the primordial spectrum [5] seem to be well described by just two numbers,

$$\Delta_{\mathcal{R}}^2(k) \simeq A_s \left(\frac{k}{k_*}\right)^{n_s-1}, A_s = (2.105 \pm 0.030) \times 10^{-9}, n_s = 0.9665 \pm 0.0038, \quad (2)$$

where the pivot is $k_* = 0.05 \text{ Mpc}^{-1}$.

If relation (2) is correct then we can reconstruct the inflationary geometry in terms of A_s , n_s and the still unknown tensor-to-scalar ratio $r_* < 0.07$ [6]. Expressing the first slow roll parameter $\epsilon(n)$ and the Hubble parameter $H(n)$ in terms of the number of e-foldings $\Delta n \equiv n - n_*$ since the pivot mode experienced horizon crossing, the lowest order slow roll approximation gives,

$$\epsilon(n) \simeq \frac{r_*}{16} e^{(1-n_s)\Delta n}, \quad H(n) \simeq H_* \exp\left[-\frac{r_*}{16(1-n_s)} \left(e^{(1-n_s)\Delta n} - 1\right)\right], \quad (3)$$

where $8\pi G H_*^2 \equiv r_* A_s \pi^2 / 2$. Using the standard procedure for reconstructing the inflaton and its potential [7–12] we find,

$$\sqrt{8\pi G} \left(\varphi(n) - \varphi_*\right) \equiv \Delta\psi \simeq -\frac{1}{1-n_s} \sqrt{\frac{r_*}{2}} \left[e^{\frac{1}{2}(1-n_s)\Delta n} - 1\right], \quad (4)$$

$$(8\pi G)^2 V(\varphi) \simeq \frac{3}{2} \pi^2 r_* A_s \exp\left[\sqrt{\frac{r_*}{8}} \Delta\psi - \left(\frac{1-n_s}{4}\right) \Delta\psi^2\right]. \quad (5)$$

Nature is under no compulsion to comply with human aesthetic prejudices, so the featureless, gently sloping potential (5) may be all there is to primordial inflation. However, it raises severe issues with the fine-tuning of initial conditions needed to make inflation start, and with the tendency

for small fluctuations to produce dramatically different conditions in distant portions of the universe [13]. What to make of this has provoked controversy even among some of the pioneers of inflation [14–16].

The power spectrum data [17] actually provides marginal evidence for more structure in the form of “features”. These are transient fluctuations away from the best fit — usually a depression of power followed by an excess at smaller angular scales — which are visible in the Planck residuals for $20 \lesssim \ell \lesssim 1500$ [18]. These were first noticed in WMAP data [19–21] and have persisted [22, 23]. None of the observed features reaches the 5σ level of a detection, but it is conceivable that this threshold might be reached by correlating them with other data sets [24]. We have suggested the possibility of doing this (in the far future) with data from the tensor power spectrum [25, 26]. Here we study the prospects for exploiting non-Gaussianity.

Maldacena’s analysis [27] established that single-scalar inflation (1) cannot produce a detectable level of non-Gaussianity if the potential is smooth like (5). The effect from a smooth potential is widely distributed over the angular bi-spectrum so the standard estimators average over all possible 3-point correlators in order to maximize the signal [28, 29]. Planck has not seen a statistically significant indication of non-Gaussianity using any of these standard estimators [30]. On the other hand, it has long been recognized that much stronger transient effects can come from features [31–33]. Because these effects are concentrated at certain angular scales the standard estimators do not resolve them well. An approximate computation of the effect from the first feature indicated that its non-Gaussian signal is not detectable [31]. We will re-examine this problem using some recently developed improvements in approximating the scalar mode functions [26, 34], and a different estimation of the signal-to-noise ratio. In spite of some technical improvements, the signal is still about 200 times too weak to be resolved.

This paper consists of six sections, of which this Introduction is the first. Section 2 is devoted to notation and conventions. The various contributions to non-Gaussianity are listed there, and the one associated with features is identified. In section 3 we apply our approximation for the scalar mode function to derive an analytic expression for the bi-spectrum as a functional of the inflationary geometry. Section 4 optimizes the parameters for a simple model of the first feature in which the bi-spectrum can be computed exactly. In section 5 this result is used to evaluate a non-standard estimator which is designed to bring out the non-Gaussianity from a feature. Our conclusions comprise section 6.

2 Notation and Conventions

Our purpose is to elucidate how quantities depend *functionally* on the geometry of inflation. We employ the Hubble representation [35] using Hubble parameter H and first slow roll parameter ϵ of the homogeneous, isotropic and spatially flat background geometry of inflation,

$$ds^2 = -dt^2 + a^2(t)d\vec{x}\cdot d\vec{x} \implies H \equiv \frac{\dot{a}}{a} > 0 \quad , \quad \epsilon \equiv -\frac{\dot{H}}{H^2} < 1 . \quad (6)$$

It is convenient to regard our time variable as $n \equiv \ln[a(t)/a_i]$, the number of e-foldings from the *beginning* of inflation. If inflation ends after n_e e-foldings then the more familiar number of e-foldings *until* the end of inflation is $N \equiv n_e - n$. With this time variable $\epsilon(n)$ provides the simplest representation for the geometry of inflation with the Hubble parameter evolved from its initial value h_i ,

$$H(n) = H_i \exp\left[-\int_0^n dm \epsilon(m)\right] . \quad (7)$$

We use a prime to denote differentiation with respect to n , as in $\epsilon = -H'/H$.

The key unknown in computing both the scalar power spectrum and the bi-spectrum is the scalar mode function $v(n, k)$. In our notation its equation, Wronskian normalization and asymptotically early time form are [36, 37],

$$v'' + \left(3 - \epsilon + \frac{\epsilon'}{\epsilon}\right)v' + \frac{k^2 v}{H^2 a^2} = 0 \quad , \quad vv'^* - v'v^* = \frac{i}{\epsilon H a^3} \quad , \quad v \longrightarrow \frac{\exp[-ik \int_0^n \frac{dm}{Ha}]}{\sqrt{2k\epsilon a^2}} . \quad (8)$$

Let n_k stand for the e-folding of first horizon crossing, when modes of wave number k obey $k \equiv H(n_k)a(n_k)$. One can see from (8) that the mode function rapidly approaches a constant after this time. The scalar power spectrum is computed by evolving $v(n, k)$ from its early time form to this constant,

$$\Delta_{\mathcal{R}}^2(k) = 4\pi G \times \frac{k^3}{2\pi^2} \times \left|v(n, k)\right|_{n \gg n_k}^2 . \quad (9)$$

Maldacena's expression for the bi-spectrum [27] can be expressed as the sum of seven contributions, of which three pairs are usually combined [33]. In our notation the $I = 1, \dots, 7$ contributions each take the form,

$$B_I(k_1, k_2, k_3) = (4\pi G)^2 \operatorname{Re} \left[v(n_e, k_1)v(n_e, k_2)v(n_e, k_3) \right. \\ \left. \times i \int_0^{n_e} dn \epsilon(n) H(n) a^3(n) \times \mathcal{B}_I^*(n, k_1, k_2, k_3) \right] . \quad (10)$$

The four unconjugated $\mathcal{B}_I(n, k_1, k_2, k_3)$ combinations are,

$$\mathcal{B}_{1+3} = \epsilon \left[\frac{K_{123}^4}{k_2^2 k_3^2} v_1 v_2' v_3' + \frac{K_{231}^4}{k_3^2 k_1^2} v_1' v_2 v_3' + \frac{K_{312}^4}{k_1^2 k_2^2} v_1' v_2' v_3 \right], \quad (11)$$

$$\mathcal{B}_2 = \epsilon \left[\left(\frac{k_1^2 + k_2^2 + k_3^2}{H^2 a^2} \right) v_1 v_2 v_3 \right], \quad (12)$$

$$\mathcal{B}_{5+6} = \epsilon^2 \left[\frac{K^4}{k_2^2 k_3^2} v_1 v_2' v_3' + \frac{K^4}{k_3^2 k_1^2} v_1' v_2 v_3' + \frac{K^4}{k_1^2 k_2^2} v_1' v_2' v_3 \right], \quad (13)$$

$$\mathcal{B}_{4+7} = \frac{\epsilon'}{\epsilon} \left[\left(\frac{k_1^2 + k_2^2 + k_3^2}{H^2 a^2} \right) v_1 v_2 v_3 - v_1 v_2' v_3' - v_1' v_2 v_3' - v_1' v_2' v_3 \right], \quad (14)$$

where the 4th order momentum factors in (11) and (13) are,

$$K_{123}^4 \equiv k_1^2(k_2^2 + k_3^2) + 2k_2^2 k_3^2 - (k_2^2 - k_3^2)^2, \quad (15)$$

$$K^4 \equiv k_1^4 + k_2^4 + k_3^4 - 2k_1^2 k_2^2 - 2k_2^2 k_3^2 - 2k_3^2 k_1^2. \quad (16)$$

Two things are apparent from the initial factors of ϵ in expressions (11-14). First, non-Gaussianity is small for smooth potentials like (5) because ϵ is small and varies slowly. From (3) we see that $\epsilon \sim \frac{1}{16} r_* < 0.0044$, and even the factor of ϵ'/ϵ in (14) is $1 - n_s \sim 0.034$. Second, much larger non-Gaussianity can arise from \mathcal{B}_{4+7} in models with features. In that case ϵ remains small, but ϵ'/ϵ can reach order one over a small range of n .

The mode-dependent factors inside the square brackets of (11-14) are also informative when combined with three insights from the mode equation (8):

1. The mode function $v(n, k)$ is oscillatory and falling off like $1/a$ until it freezes in to a constant $V(k)$ (which might be complex) around $n \approx n_k$;
2. The approach to $V(k)$ has real part $\text{Re}[v(n, k)/V(k)] \sim (k/Ha)^2$; and
3. The approach has $\text{Im}[v(n, k)/V(k)] \sim -1/2\epsilon Ha^3 |V(k)|^2$.

Together with the general form (10), these facts imply that the n -integrand for each of the four contributions is oscillatory before the largest of the three wave numbers has experienced horizon crossing and falls off like $1/a^2$ thereafter. This has important consequences for designing estimators to detect non-Gaussianity. When the potential is smooth both $\epsilon(n)$ and $\partial_n \ln[\epsilon]$ are nearly constant, so all wave numbers will show nearly the same effect and the best strategy is to combine them as the standard estimators do. However,

when a feature is present the factor of $\partial_n \ln[\epsilon(n)]$ in (14) becomes significant in small range of n , and the non-Gaussian signal will be much larger for modes which experience horizon crossing around that time. Averaging over all observable wave numbers runs the risk of drowning a real signal in noise.

Because conventions differ we close by reviewing how the fundamental fields relate to $\Delta_{\mathcal{R}}^2(k)$ and $B(k_1, k_2, k_3)$. We use the gauge of Salopek, Bond and Bardeen [38] in which time is fixed by setting the inflaton to its background value and the graviton field is transverse. In this gauge the metric components g_{00} and g_{0i} are constrained and the dynamical variables $\zeta(n, \vec{x})$ and $h_{ij}(n, \vec{x})$ reside in the spatial components,

$$g_{ij}(n, \vec{x}) = a^2 e^{2\zeta(n, \vec{x})} \times \left[e^{h(n, \vec{x})} \right]_{ij} \quad , \quad h_{ii}(n, \vec{x}) = 0 . \quad (17)$$

Scalar perturbations derive from $\zeta(n, \vec{x})$ whose free field expansion is,

$$\tilde{\zeta}(n, \vec{k}) \equiv \int d^3x e^{-i\vec{k}\cdot\vec{x}} \zeta(n, \vec{x}) = \sqrt{4\pi G} \left[v(n, k) \alpha(\vec{k}) + v^*(n, k) \alpha^\dagger(-\vec{k}) \right] , \quad (18)$$

where α^\dagger and α are creation and annihilation operators,

$$\left[\alpha(\vec{k}), \alpha^\dagger(\vec{p}) \right] = (2\pi)^3 \delta^3(\vec{k} - \vec{p}) \quad , \quad \alpha(\vec{k}) \Big| \Omega \rangle = 0 . \quad (19)$$

Assuming the wave numbers experience horizon crossing before the end of inflation n_e , our power spectrum and bi-spectrum are,

$$\left\langle \Omega \left| \tilde{\zeta}(n_e, \vec{k}) \tilde{\zeta}(n_e, \vec{p}) \right| \Omega \right\rangle = \frac{2\pi^2}{k^3} \times \Delta_{\mathcal{R}}^2(k) \times (2\pi)^3 \delta^3(\vec{k} + \vec{p}) , \quad (20)$$

$$\left\langle \Omega \left| \tilde{\zeta}(n_e, \vec{k}_1) \tilde{\zeta}(n_e, \vec{k}_2) \tilde{\zeta}(n_e, \vec{k}_3) \right| \Omega \right\rangle = B(k_1, k_2, k_3) \times (2\pi)^3 \delta^3(\vec{k}_1 + \vec{k}_2 + \vec{k}_3) . \quad (21)$$

Note that while the power spectrum is dimensionless, the bi-spectrum has the dimension of k^6 .

3 Analytic Approximation for the Bi-Spectrum

In this section we first convert the key contribution (14) from the mode function $v(n, k)$ to its norm-square $N(n, k)$. Then we introduce an approximation [26, 34] which should be very accurate for the physically relevant case of small $\epsilon(n)$ but significant $\partial_n \ln[\epsilon(n)]$. Finally, we study a model of the first feature to compare our result for $B_{4+7}(k_1, k_2, k_3)$ with the simpler approximation of Adshead, Dvorkin, Hu and Peiris [31].

3.1 Approximating the mode functions

Even considered as a purely numerical problem, it is better to convert the equations (8) for $v(n, k)$ into relations for $N(n, k) \equiv |v(n, k)|^2$ [39]. Avoiding the need to keep track of the phase makes about a quadratic improvement in convergence. Further, nothing is lost because the phase can be recovered by a simple integration [26],

$$v(n, k) = \sqrt{N(n, k)} \exp\left[-i \int_0^n \frac{dm}{2\epsilon H a^3 N}\right] \equiv \sqrt{N(n, k)} e^{i\theta(n, k)}. \quad (22)$$

It is best to begin with the outer factors of $v(n_e, k)$ in expression (10). Assuming the various wave numbers have experienced horizon crossing these outer mode functions can be expressed in terms of the power spectrum (9),

$$v(n_e, k) = \sqrt{\frac{\pi}{2Gk^3}} \Delta_{\mathcal{R}}(k) e^{i\theta(n_e, k)}. \quad (23)$$

We next combine each outer phase with the appropriate inner phase,

$$\widehat{v}(n, k) \equiv v(n, k) e^{-i\theta(n_e, k)} \implies \theta(n, k) - \theta(n_e, k) = \int_n^{n_e} \frac{dm}{\epsilon H a^3 N} \equiv \phi(n, k). \quad (24)$$

Note that $\phi(n, k)$ approaches zero like $1/a^3$ for large n . At this stage one can recognize the real part of the undifferentiated terms,

$$\text{Re}\left[i \widehat{v}_1^* \widehat{v}_2^* \widehat{v}_3^*\right] = \sqrt{N_1 N_2 N_3} \sin(\phi_1 + \phi_2 + \phi_3). \quad (25)$$

The differentiated terms are more complicated,

$$\widehat{v}'(n, k) = \widehat{v}(n, k) \left[\frac{N'(n, k)}{2N(n, k)} + i\phi'(n, k) \right]. \quad (26)$$

Hence we have,

$$\begin{aligned} \text{Re}\left[i \widehat{v}_1^* \widehat{v}_2'^* \widehat{v}_3'^*\right] = \sqrt{N_1 N_2 N_3} \left\{ \sin(\phi_1 + \phi_2 + \phi_3) \left[\frac{N'_2}{2N_2} \frac{N'_3}{2N_3} - \phi'_2 \phi'_3 \right] \right. \\ \left. + \cos(\phi_1 + \phi_2 + \phi_3) \left[\frac{N'_2}{2N_2} \phi'_3 + \frac{N'_3}{2N_3} \phi'_2 \right] \right\}. \quad (27) \end{aligned}$$

There are three terms such as (27), so putting everything together gives,

$$\begin{aligned}
B_{4+7}(k_1, k_2, k_3) &= \frac{4\pi^4 \Delta_{\mathcal{R}}(k_1) \Delta_{\mathcal{R}}(k_2) \Delta_{\mathcal{R}}(k_3)}{k_1^2 k_2^2 k_3^2} \times \sqrt{\frac{2Gk_1 k_2 k_3}{\pi}} \int_0^{n_e} dn \epsilon' H a^3 \\
&\times \sqrt{N_1 N_2 N_3} \left\{ \sin(\phi_1 + \phi_2 + \phi_3) \left[\left(\frac{k_1^2 + k_2^2 + k_3^2}{H^2 a^2} \right) - \frac{N'_2}{2N_2} \frac{N'_3}{2N_3} + \phi'_2 \phi'_3 - \dots \right] \right. \\
&\quad \left. - \cos(\phi_1 + \phi_2 + \phi_3) \left[\frac{N'_1}{2N_1} (\phi'_2 + \phi'_3) + \frac{N'_2}{2N_2} (\phi'_3 + \phi'_1) + \frac{N'_3}{2N_3} (\phi'_1 + \phi'_2) \right] \right\}. \quad (28)
\end{aligned}$$

To develop a useful approximation for (28) we first factor $N(n, k)$ into the instantaneously constant ϵ solution $N_0(n, k)$ times the exponential of a residual $g(n, k)$ which is sourced by derivatives of $\ln[\epsilon(n)]$ [26, 34],

$$N(n, k) = N_0(n, k) \times \exp \left[-\frac{1}{2} g(n, k) \right]. \quad (29)$$

Of course the derivatives of $\ln[\epsilon(n)]$ which source $g(n, k)$ are of great concern in the study of features, as is the potentially large factor of $1/\epsilon$ in $N_0(n, k)$. Taking all the other factors of ϵ to zero causes a negligible loss of accuracy. The resulting approximation involves three functions $\tilde{g}(n, n_k)$, $\tilde{\gamma}'(n, n_k)$ and $\tilde{\phi}(n, n_k)$ which must be tabulated over a narrow range of n and n_k ,

$$\begin{aligned}
\tilde{B}_{4+7}(k_1, k_2, k_3) &= \frac{4\pi^4 \Delta_{\mathcal{R}}(k_1) \Delta_{\mathcal{R}}(k_2) \Delta_{\mathcal{R}}(k_3)}{k_1^2 k_2^2 k_3^2} \times - \int_0^{n_e} dn \partial_n \sqrt{\frac{GH^2(n)}{\pi \epsilon(n)}} \\
&\times \sqrt{(1+e^{2\Delta n_1})(1+e^{2\Delta n_2})(1+e^{2\Delta n_3})} e^{-\frac{1}{2}(\tilde{g}_1 + \tilde{g}_2 + \tilde{g}_3)} \left\{ \sin(\tilde{\phi}_1 + \tilde{\phi}_2 + \tilde{\phi}_3) \right. \\
&\quad \times \left[e^{-2\Delta n_1} - \left(\frac{1}{1+e^{2\Delta n_2}} + \frac{1}{4} \tilde{\gamma}'_2 \right) \left(\frac{1}{1+e^{2\Delta n_3}} + \frac{1}{4} \tilde{\gamma}'_3 \right) + \tilde{\phi}'_2 \tilde{\phi}'_3 + (231) + (312) \right] \\
&\quad \left. - \cos(\tilde{\phi}_1 + \tilde{\phi}_2 + \tilde{\phi}_3) \left[\left(\frac{1}{1+e^{2\Delta n_1}} + \frac{1}{4} \tilde{\gamma}'_1 \right) (\tilde{\phi}'_2 + \tilde{\phi}'_3) + (231) + (312) \right] \right\}. \quad (30)
\end{aligned}$$

Here and henceforth $\Delta n_i \equiv n - n_i$, where n_i is the e-folding at which wave number k_i experiences horizon crossing.

The tabulated function $\tilde{g}(n, n_k)$ represents an approximation of the amplitude residual $g(n, k)$ in (29). It is expressed as a Green's function integral over sources before and after horizon crossing,

$$S_b(m) = \partial_m^2 \ln[\epsilon(m)] + \frac{1}{2} \left(\partial_m \ln[\epsilon(m)] \right)^2 + 3 \partial_m \ln[\epsilon(m)], \quad (31)$$

$$S_a(m, n_k) = \frac{2\partial_m \ln[\epsilon(m)]}{1+e^{2\Delta m}} + \left(\frac{2e^{-\Delta m} \frac{\epsilon(n_k)}{\epsilon(m)}}{1+e^{2\Delta m}} \right)^2, \quad (32)$$

where $\Delta m \equiv m - n_k$. The integral expression for $\tilde{G}(n, n_k)$ is,

$$\begin{aligned} \tilde{g}(n, n_k) = & -2\theta(-\Delta n) \int_0^n dm G(\Delta m, \Delta n) S_b(m) + 2\theta(\Delta n) \left\{ G(0, \Delta n) \frac{\epsilon'(n_k)}{\epsilon(n_k)} \right. \\ & \left. - \int_0^{n_k} dm G(\Delta m, \Delta n) S_b(m) - \int_{n_k}^n dm G(\Delta m, \Delta n) S_a(m, n_k) \right\}, \quad (33) \end{aligned}$$

where the Green's function is,

$$\begin{aligned} G(\Delta m, \Delta n) = & \frac{1}{2} (e^{\Delta m} + e^{3\Delta m}) \\ & \times \sin \left[2e^{-\Delta m} - 2 \tan^{-1}(e^{-\Delta m}) - 2e^{-\Delta n} + 2 \tan^{-1}(e^{-\Delta n}) \right]. \quad (34) \end{aligned}$$

Differentiating the Green's function with respect to n gives,

$$\begin{aligned} \partial_n G(\Delta m, \Delta n) = & \left(\frac{e^{\Delta m} + e^{3\Delta m}}{e^{\Delta n} + e^{3\Delta n}} \right) \\ & \times \cos \left[2e^{-\Delta m} - 2 \tan^{-1}(e^{-\Delta m}) - 2e^{-\Delta n} + 2 \tan^{-1}(e^{-\Delta n}) \right]. \quad (35) \end{aligned}$$

It occurs in the second of the tabulated functions,

$$\tilde{\gamma}'(n, n_k) = 2\theta(-\Delta n) \partial_n \ln[\epsilon(n)] + \partial_n \tilde{g}(n, n_k). \quad (36)$$

The final tabulated function is our approximation of the angle $\phi(n, k)$,

$$\tilde{\phi}(n, n_k) = \int_n^{n_e} dm \frac{e^{-\Delta m + \frac{1}{2}\tilde{g}(m, n_k)}}{1+e^{2\Delta m}}. \quad (37)$$

Note that its derivative does not require separate tabulation,

$$\tilde{\phi}'(n, n_k) = -\frac{e^{-\Delta n + \frac{1}{2}\tilde{g}(n, n_k)}}{1+e^{2\Delta n}}. \quad (38)$$

Adshead, Dvorkin, Hu and Peiris [31] introduced a much simpler approximation which, in our language, corresponds to setting $\tilde{g}(n, n_k)$ and $\tilde{\gamma}'(n, k)$

to zero in expression (30). Note that this reduces the angle and its derivative to be functions of just the single variable $\Delta n = n - n_k$,

$$\tilde{\phi}(n, n_k) \Big|_{\tilde{g}=0} = e^{-\Delta n} - \tan^{-1}\left(e^{-\Delta n}\right) \quad , \quad \tilde{\phi}'(n, n_k) \Big|_{\tilde{g}=0} = -\frac{e^{-\Delta n}}{1+e^{2\Delta n}} . \quad (39)$$

This approximation is certainly simpler to implement, but it completely ignores how the inner mode functions change in response to the feature.

3.2 The Step Model

The model we shall study belongs to a class introduced in 2001 by Adams, Cresswell and Easther [40],

$$V(\varphi) = \frac{1}{2}m^2\varphi^2 \times \left[1 + c \tanh\left(\frac{\varphi-b}{d}\right)\right] . \quad (40)$$

A fit to the first feature ($20 \lesssim \ell \lesssim 40$) using WMAP data gave [41],

$$b = \frac{14.668}{\sqrt{8\pi G}} \quad , \quad c = 1.505 \times 10^{-3} \quad , \quad d = \frac{0.02705}{\sqrt{8\pi G}} \quad , \quad m = \frac{7.126 \times 10^{-6}}{\sqrt{8\pi G}} . \quad (41)$$

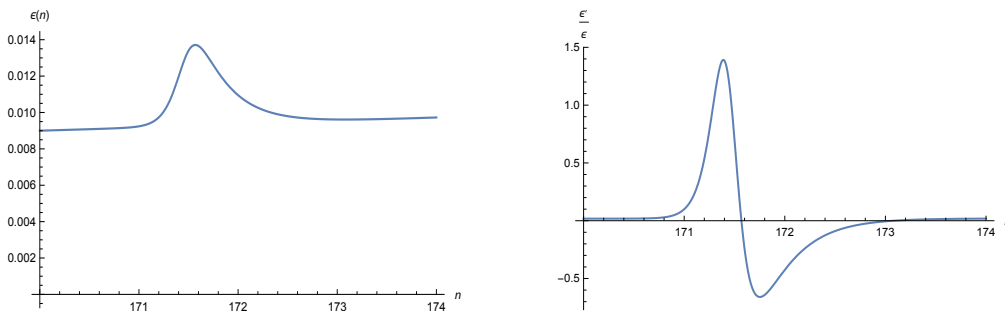


Figure 1: The left hand graph gives $\epsilon(n)$ for the Step Model (40-41). The right hand graph shows $\partial_n \ln[\epsilon(n)]$ for this model. Note that the logarithmic derivative is only significant in the narrow range $170.8 \lesssim n \lesssim 172.8$.

Figure 1 shows the first slow roll parameter and its logarithmic derivative for this model. Two obvious points are:

1. The first slow roll parameter is always very small;¹ and

¹ It is actually a little too large for the improved bounds on the tensor-to-scalar ratio [6] since the time of WMAP. However, the model serves well enough for the purposes of illustration.

2. The crucial factor of $\partial_n \ln[\epsilon(n)]$ which sources non-Gaussianity is only significant for the two e-foldings $170.8 \lesssim n \lesssim 172.8$.

Inflation ends for this model at $n_e \simeq 225.6$ so the feature peaks about 54 e-foldings before the end of inflation.

Let us first establish that our approximations for the amplitude correction (33) and for the phase (37) are valid. Figure 2 displays the exact results (in blue) versus our approximations (in yellow) for the case of $n_k = 172.5$ where the amplitude correction is close to its maximum. The agreement is good, except for an offset at late times which is due to $g(n, k)$ having become large enough around $n \approx 172$ that nonlinear corrections matter [34]. For most values of n_k this is not an issue and, even for $n_k = 172.5$, the rightmost graph of Fig. 1 shows that the offset has little effect on non-Gaussianity.

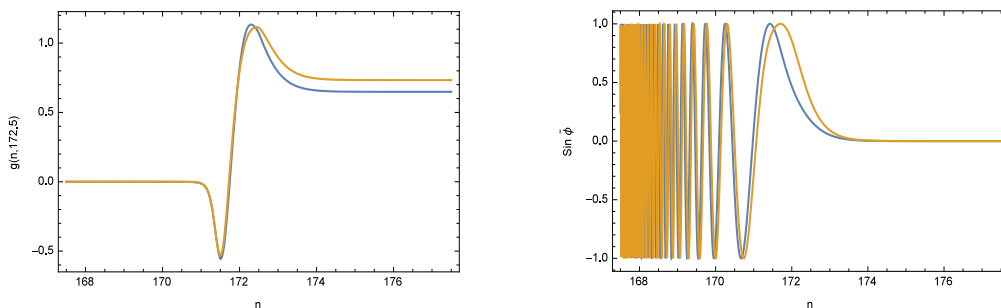


Figure 2: Comparison between exact results (in blue) and our approximations (in yellow) for the amplitude correction (33) and the phase (37). The left hand graph shows $g(n, k)$ and the right hand graph shows $\sin[\tilde{\phi}(n, k)]$.

In view of point (2) above, we only require the tabulated functions $\tilde{g}(n, n_k)$, $\tilde{\gamma}'(n, n_k)$ and $\tilde{\phi}(n, n_k)$ for the two e-foldings from $n = 170.8$ to $n = 172.8$. Figure 3 shows contour plots of these functions for modes which experience horizon crossing in the range $170 < n_k < 173.5$.

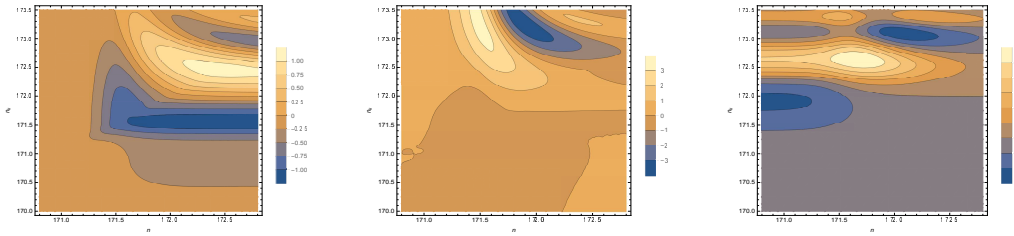


Figure 3: Various correction factors for the Step Model. The left hand graph gives our approximation (33) for $(-4 \text{ times the logarithm of})$ the amplitude correction $g(n, n_k)$ in the Step Model. The middle graph shows the derivative factor (36). And the right hand graph shows how much our approximation (37) differs from the de Sitter result (39).

It is important to bear in mind that the source $\partial_n \ln[\epsilon(n)]$ on Fig. 1 modulates how the corrections of Fig. 3 affect non-Gaussianity. So although the graph of $\tilde{g}(n, n_k)$ shows a strong amplitude enhancement for $n_k \simeq 171.5$, and an equally strong suppression for $n_k \simeq 172.5$, the latter effect is much less significant because it peaks for $n \gtrsim 172.1$, by which point $\partial_n \ln[\epsilon(n)]$ is small. Because of this modulation, the biggest correction comes from the large positive phase shift at $n_k \simeq 172.6$, which peaks at $n \simeq 171.7$.

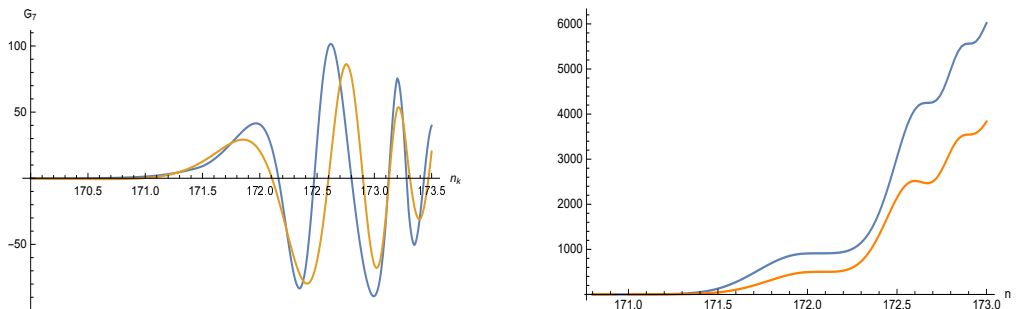


Figure 4: The left hand graph shows the “inner” part of expression (30), starting from $-\int_0^{n_e} dn \dots$, for the equilateral triangle case of $k_1 = k_2 = k_3$. The blue curve shows our approximation while the yellow curve shows the simpler approximation of Adshead, Dvorkin, Hu and Peiris [31]. The right hand graph shows the integral of the square of our approximation (in blue) versus the product of our approximation times theirs (in yellow). The ratio of the areas under the yellow to the blue curves is about 0.637 at the end.

Figure 4 gives some idea of the significance of the various corrections we have introduced to the approximation of Adshead, Dvorkin, Hu and Peiris [31]. We will see in section 5 that the best estimator consists of a weighted sum over observations of the observed result multiplied by the the-

oretical prediction. For the sort of oscillatory signal expected from features *this sort of estimator will only be reliable when the theoretical prediction is accurate*. Actual observations are made in the 2-dimensional space of right ascension and declination, rather than the 3-dimensional wave vector, and the estimator includes data from all orientations, not just the equilateral triangle configuration which the figure displays. However, a rough idea of how much an inaccurate prediction can degrade the signal can be gained by comparing the indefinite integral of the square of our prediction with the indefinite integral of the production of our prediction times the approximation of Adshead, Dvorkin, Hu and Peiris. Although this approximation gets the general shape and amplitude right, employing it would degrade the signal by a factor of 0.637.

4 The Square Well Model

In 1992 Starobinsky proposed a simple model in which the first slow roll parameter makes an instantaneous jump from one value to another, which permits the mode functions to be solved exactly [42]. Because the fundamental source of non-Gaussianity $\partial_n \ln[\epsilon(n)]$ is a delta function for this case, one can exactly compute $B_{4+7}(k_1, k_2, k_3)$ and derive excellent approximations for the remaining contributions [43–45]. We shall make a slight modification of this model in which $\epsilon(n)$ returns to its original value after a short number of e-foldings Δn ,

$$\epsilon(n) = \epsilon_1 \theta(n_0 - n) + \epsilon_2 \theta(n - n_0) \theta(n_0 + \Delta n - n) + \epsilon_1 \theta(n - n_0 - \Delta n). \quad (42)$$

We first solve exactly for the mode functions. Next a determination is made of the parameter values for n_0 , Δn , ϵ_1 and ϵ_2 to cause the scalar power spectrum of this model to agree with a numerical determination of the Step Model power spectrum of section 3.2 over the crucial range $170.8 < n_k < 172.8$. After that $B_{4+7}(k_1, k_2, k_3)$ is computed exactly, and then in the approximation of setting all small factors of ϵ to zero.

For $\epsilon(n) = \epsilon_i$ for all time then the exact mode function is,

$$v_i(n, k) = \sqrt{\frac{\pi}{4\epsilon_i(1-\epsilon_i)Ha^3}} H_{\nu_i}^{(1)}\left(\frac{k}{(1-\epsilon_i)Ha}\right), \quad \nu_i = \frac{1}{2}\left(\frac{3-\epsilon_i}{1-\epsilon_i}\right). \quad (43)$$

For the actual parameter (42) the mode function takes the form,

$$v(n, k) = v_1(n, k) \theta(n_0 - n)$$

$$+v_B(n, k)\theta(n-n_0)\theta(n_0+\Delta n-n) + v_C(n, k)\theta(n-n_0-\Delta n) , \quad (44)$$

where $v_B(n, k)$ and $v_C(n, k)$ are,

$$v_B(n, k) = \alpha v_2(n, k) + \beta v_2^*(n, k) , \quad (45)$$

$$v_C(n, k) = \alpha \left[\gamma v_1(n, k) + \delta v_1^*(n, k) \right] + \beta \left[\gamma v_1(n, k) + \delta v_1^*(n, k) \right]^* . \quad (46)$$

The appropriate matching conditions at $n = n_0$ and $n = n_0 + \Delta n$ are the continuity of $v(n, k)$ and of the product $\epsilon(n) \times v'(n, k)$. The coefficients α and β involve the mode functions (43) and their derivatives evaluated at $n = n_0$,

$$\alpha = -iHa^3 \left[\epsilon_2 v_1 v_2'^* - \epsilon_1 v_1' v_2^* \right] , \quad \beta = iHa^3 \left[\epsilon_2 v_1 v_2' - \epsilon_1 v_1' v_2 \right] . \quad (47)$$

The coefficients γ and δ involve the mode functions (43) and their derivatives evaluated at $n = n_0 + \Delta n$,

$$\gamma = -iHa^3 \left[\epsilon_1 v_2 v_1'^* - \epsilon_2 v_2' v_1^* \right] , \quad \delta = iHa^3 \left[\epsilon_1 v_2 v_1' - \epsilon_2 v_2' v_1 \right] . \quad (48)$$

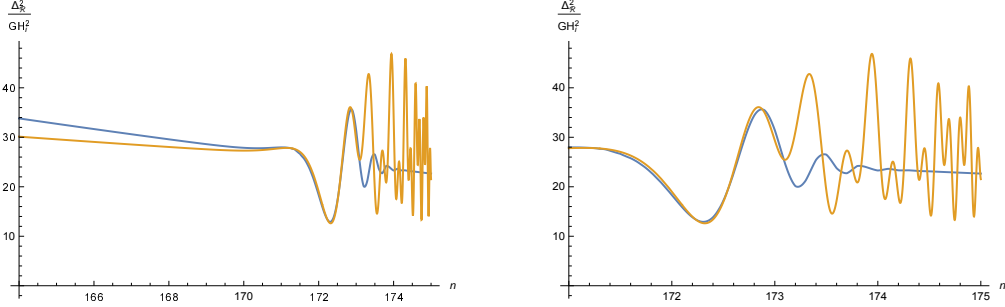


Figure 5: Both graphs show the $\Delta_{\mathcal{R}}^2(k)$ as a function of e-folding of horizon crossing, for the Step Model (in blue) and for the best fit Square Well Model (in yellow).

From expression (46) and the small argument form of the Hankel function we infer the late time limit of the mode function,

$$\lim_{n \gg n_k} v_C(n, k) = -\frac{iH(n_k)}{\sqrt{2\epsilon_1 k^3}} \times \frac{\Gamma(\nu_1) [2(1-\epsilon_1)]^{\frac{1}{1-\epsilon_1}}}{\sqrt{\pi}} \times \left[\alpha(\gamma-\delta) - \beta(\gamma^*-\delta^*) \right] . \quad (49)$$

Substituting this in expression (9) gives the Square Well model's prediction for the scalar power spectrum,

$$\Delta_{\mathcal{R}}^2(k) = \frac{GH^2(n_k)}{\pi\epsilon_1} \times \frac{\Gamma^2(\nu_1) [2(1-\epsilon_1)]^{\frac{2}{1-\epsilon_1}}}{\pi} \times \left| \alpha(\gamma-\delta) - \beta(\gamma^*-\delta^*) \right|^2 . \quad (50)$$

Figure 5 compares (50) with a numerical determination of $\Delta_{\mathcal{R}}^2(k)$ for the Step Model. There is no way to make the two results agree for all values of n_k , however, very good concurrence over the key range of $170.8 < n_k < 172.8$ results from the following choices for the Square Well parameters,

$$n_0 = 171.3 \quad , \quad \Delta n = 0.7 \quad , \quad \epsilon_1 = 0.0093 \quad , \quad \epsilon_2 = 0.0137 \quad . \quad (51)$$

The infinite sequence of oscillations (“ringing”) evident in Fig. 5 is the result of the sharp transitions in $\epsilon(n)$ for the Square Well Model (42). For smooth transitions, such as those of the Step Model, the oscillations decay rapidly. Of course no one understands what caused features (if they are present) so it may be that the transition really *is* instantaneous, in which case ringing is a prominent signature that persists long after the transition. This possibility was pursued in a fascinating study by Adshead, Dvorkin, Hu and Lim [32]. However, we shall here take the view that ringing is an artifact of modelling smooth transitions as instantaneous, and we shall accordingly focus narrowly on the two e-foldings $170.8 < n_k < 172.8$ over which the Square Well model is in reasonable agreement with the Step Model.

The great advantage of the Square Well Model is that the key modulation factor of ϵ'/ϵ in expression (14) is a delta function,

$$\frac{\epsilon'(n)}{\epsilon(n)} = \ln\left(\frac{\epsilon_2}{\epsilon_1}\right) \left[\delta(n-n_0) - \delta(n-n_1) \right] \quad , \quad (52)$$

where $n_1 \equiv n_0 + \Delta n$. We must also understand how to evaluate certain discontinuous factors at the jumps,

$$\epsilon(n_0) \longrightarrow \left(\frac{\epsilon_1 + \epsilon_2}{2}\right) \longleftarrow \epsilon(n_1) \quad , \quad (53)$$

$$\epsilon(n_0)v'(n_0, k_\alpha)v'(n_0, k_\beta) \longrightarrow \left(\frac{\epsilon_1 + \epsilon_2}{2}\right) \frac{\epsilon_1}{\epsilon_2} v'_1(n_0, k_\alpha)v'_1(n_0, k_\beta) \quad , \quad (54)$$

$$\epsilon(n_1)v'(n_1, k_\alpha)v'(n_1, k_\beta) \longrightarrow \left(\frac{\epsilon_1 + \epsilon_2}{2}\right) \frac{\epsilon_2}{\epsilon_1} v'_B(n_1, k_\alpha)v'_B(n_1, k_\beta) \quad . \quad (55)$$

Substituting relations (52) and (53-55) into expressions (10) and (14) gives,

$$B_{4+7}(k_1, k_2, k_3) = (4\pi G)^2 \left(\frac{\epsilon_1 + \epsilon_2}{2}\right) \ln\left(\frac{\epsilon_2}{\epsilon_1}\right) \text{Re} \left[i v_C(n_e, k_1) v_C(n_e, k_2) v_C(n_e, k_3) \right. \\ \left. \times \left[H(n_0) a^3(n_0) F^*(n_0, k_1, k_2, k_3) - H(n_1) a^3(n_1) G^*(n_1, k_1, k_2, k_3) \right] \right] \quad , \quad (56)$$

where the upper and lower factors are,

$$\begin{aligned}
F(n, k_1, k_2, k_3) &\equiv \frac{(k_1^2 + k_2^2 + k_3^2)}{H^2(n)a^2(n)} v_1(n, k_1)v_1(n, k_2)v_1(n, k_3) \\
&\quad - \frac{\epsilon_1}{\epsilon_2} v_1(n, k_1)v_1'(n, k_2)v_1'(n, k_3) - \frac{\epsilon_1}{\epsilon_2} v_1'(n, k_1)v_1(n, k_2)v_1'(n, k_3) \\
&\quad \quad \quad - \frac{\epsilon_1}{\epsilon_2} v_1'(n, k_1)v_1'(n, k_2)v_1(n, k_3) , \quad (57)
\end{aligned}$$

$$\begin{aligned}
G(n, k_1, k_2, k_3) &\equiv \frac{(k_1^2 + k_2^2 + k_3^2)}{H^2(n)a^2(n)} v_B(n, k_1)v_B(n, k_2)v_B(n, k_3) \\
&\quad - \frac{\epsilon_2}{\epsilon_1} v_B(n, k_1)v_B'(n, k_2)v_B'(n, k_3) - \frac{\epsilon_2}{\epsilon_1} v_B'(n, k_1)v_B(n, k_2)v_B'(n, k_3) \\
&\quad \quad \quad - \frac{\epsilon_2}{\epsilon_1} v_B'(n, k_1)v_B'(n, k_2)v_B(n, k_3) , \quad (58)
\end{aligned}$$

Expressions (56-58) are exact, but somewhat opaque because they conceal certain large factors of $1/\epsilon$, and because they are obscured by many other negligibly small positive powers of ϵ . There is no appreciable loss of accuracy, and a considerable simplification, by extracting the large factors of $1/\epsilon$ and setting the other factors of ϵ to zero. Note that this makes the Hubble parameter constant. Two ratios which involve the momenta are,

$$\kappa_i \equiv \frac{k_i}{H(n_0)a(n_0)} \longrightarrow e^{n\kappa_i - n_0} , \quad \lambda_i \equiv \frac{k_i}{H(n_1)a(n_1)} \longrightarrow e^{n\kappa_i - n_1} = \kappa_i e^{-\Delta n} . \quad (59)$$

Applying these approximations to the mode functions (at n_0 and n_1) and their first derivatives gives,

$$v_i(n_0, k) \longrightarrow -\frac{iH(1-i\kappa)e^{i\kappa}}{\sqrt{2\epsilon_i k^3}} , \quad v_i'(n_0, k) \longrightarrow \frac{iH\kappa^2 e^{i\kappa}}{\sqrt{2\epsilon_i k^3}} , \quad (60)$$

$$v_i(n_1, k) \longrightarrow -\frac{iH(1-i\lambda)e^{i\lambda}}{\sqrt{2\epsilon_i k^3}} , \quad v_i'(n_1, k) \longrightarrow \frac{iH\lambda^2 e^{i\lambda}}{\sqrt{2\epsilon_i k^3}} . \quad (61)$$

These approximations carry the first set of combination coefficients (47) to,

$$\alpha_i \longrightarrow \frac{i}{2\kappa_i} \left[(1-i\kappa_i) \sqrt{\frac{\epsilon_2}{\epsilon_1}} - (1+i\kappa_i) \sqrt{\frac{\epsilon_1}{\epsilon_2}} \right] , \quad (62)$$

$$\beta_i \longrightarrow \frac{i}{2\kappa_i} (1-i\kappa_i) \left[\sqrt{\frac{\epsilon_2}{\epsilon_1}} - \sqrt{\frac{\epsilon_1}{\epsilon_2}} \right] e^{2i\kappa_i} . \quad (63)$$

Only the difference of the second set (48) matters, and it becomes,

$$\gamma_i - \delta_i \longrightarrow \frac{e^{i\lambda_i}}{\lambda_i} \left[(1 - i\lambda_i) \sin(\lambda_i) \sqrt{\frac{\epsilon_1}{\epsilon_2}} - \left[\sin(\lambda_i) - \lambda_i \cos(\lambda_i) \right] \sqrt{\frac{\epsilon_2}{\epsilon_1}} \right]. \quad (64)$$

With these approximations expression (14) assumes the form,

$$B_{4+7}(k_1, k_2, k_3) \longrightarrow \frac{(\pi GH^2)^2}{k_1^2 k_2^2 k_3^2} \left(\frac{\epsilon_1 + \epsilon_2}{\epsilon_1^3} \right) \ln \left(\frac{\epsilon_2}{\epsilon_1} \right) \text{Re} \left[\frac{iA_1 A_2 A_3}{\kappa_1 \kappa_2 \kappa_3} \right. \\ \left. \times \left[\mathcal{F}^* e^{-i(\kappa_1 + \kappa_2 + \kappa_3)} - \left(\frac{\epsilon_1}{\epsilon_2} \right)^{\frac{3}{2}} \mathcal{G}^* e^{-i(\lambda_1 + \lambda_2 + \lambda_3)} \right] \right], \quad (65)$$

where $A_i \equiv \alpha_i(\gamma_i - \delta_i) - \beta_i(\gamma_i^* - \delta_i^*)$ and the approximated factors are,

$$\mathcal{F} = (\kappa_1^2 + \kappa_2^2 + \kappa_3^2)(1 - i\kappa_1)(1 - i\kappa_2)(1 - i\kappa_3) \\ - \frac{\epsilon_1}{\epsilon_2} \kappa_1^2 \kappa_2^2 (1 - i\kappa_3) - \frac{\epsilon_1}{\epsilon_2} \kappa_1^2 \kappa_3^2 (1 - i\kappa_2) - \frac{\epsilon_1}{\epsilon_2} \kappa_2^2 \kappa_3^2 (1 - i\kappa_1), \quad (66)$$

$$\mathcal{G} = e^{\Delta n} (\kappa_1^2 + \kappa_2^2 + \kappa_3^2) \prod_{i=1}^3 \left[\alpha_i (1 - i\lambda_i) - \beta_i (1 + i\lambda_i) e^{-2i\lambda_i} \right] \\ - e^{-\Delta n} \frac{\epsilon_2}{\epsilon_1} \sum_{i=1}^3 \left[\prod_{j \neq i} \kappa_j^2 (\alpha_j - \beta_j e^{-2i\lambda_j}) \right] \left[\alpha_i (1 - i\lambda_i) - \beta_i (1 + i\lambda_i) e^{-2i\lambda_i} \right]. \quad (67)$$

5 Estimator for the First Feature

We have so far dealt with the scalar spectrum and bi-spectrum formed from the spatial Fourier transform (18) of the primordial scalar perturbation at the end of inflation $\tilde{\zeta}(n_e, \vec{k})$. The existing data from observations of the cosmic microwave radiation differ in three ways:

1. They are made at late times, after the perturbation has experienced second horizon crossing;
2. They represent variations of intensity that are imprinted by the Sachs-Wolfe effect [46] as photons propagate through the perturbed geometry from the time of recombination to the present; and
3. They are reported as coefficients $a_{\ell m}$ of the spherical harmonic basis $Y_{\ell m}(\theta, \phi)$ whose angular coordinates represent the direction from which the radiation came.

We first explain how to convert theoretical predictions from the Fourier basis to the angular basis. We also review relations among the different ways of representing the angular bi-spectrum. This notation is employed to give an estimator for the first feature. We then explore its statistical properties assuming that there is no feature. The section closes with a computation of the estimator and its variance using Planck data.

The fundamental variables in measurements of the fractional CMB temperature variation are the spherical harmonic coefficients $a_{\ell m}$,

$$\frac{\Delta T(\theta, \phi)}{T_0} = \sum_{\ell=2}^{\infty} \sum_{m=-\ell}^{\ell} a_{\ell m} Y_{\ell m}(\theta, \phi). \quad (68)$$

They are integrals of the primordial scalar perturbation,

$$a_{\ell m} = 4\pi (-i)^\ell \int \frac{d^3 k}{(2\pi)^3} \Delta_\ell(k) Y_{\ell m}(\hat{k}) \tilde{\zeta}(n_e, \vec{k}). \quad (69)$$

Here $\Delta_\ell(k)$ is the photon transfer function needed to evolve the primordial perturbation from n_e to the time of recombination and couple it to the cosmic microwave radiation. Note that expression (69) is still a quantum operator, even though it behaves as a classical random variable because the primordial perturbation $\tilde{\zeta}(n_e, \vec{k})$ has experienced first horizon crossing. We denote its measured value by a superscript “obs”, as in $a_{\ell m}^{\text{obs}}$. We indicate theoretical predictions for the statistical properties of correlators of these random variables using an explicit expectation value. For example, the observed and predicted variances of the $a_{\ell m}$ are,

$$C_\ell^{\text{obs}} \equiv \frac{1}{2\ell+1} \sum_{m=-\ell}^{\ell} |a_{\ell m}^{\text{obs}}|^2, \quad C_\ell \equiv \frac{1}{2\ell+1} \sum_{m=-\ell}^{\ell} \langle \Omega | a_{\ell m}^* a_{\ell m} | \Omega \rangle. \quad (70)$$

Note that combining relations (20), (69) and (70) allows us to express the C_ℓ 's in terms of the power spectrum,

$$C_\ell = 4\pi \int_0^\infty \frac{dk}{k} \Delta_\ell^2(k) \Delta_{\mathcal{R}}^2(k). \quad (71)$$

We follow the notation of Fergusson and Shellard for the angular bi-spectrum [28]. The fundamental variable is the expectation value of three $a_{\ell m}$'s,

$$B_{m_1 m_2 m_3}^{\ell_1 \ell_2 \ell_3} \equiv \langle \Omega | a_{\ell_1 m_1} a_{\ell_2 m_2} a_{\ell_3 m_3} | \Omega \rangle. \quad (72)$$

Assuming isotropy, which we shall always do, this can be expressed in terms of a reduced angular bi-spectrum $b_{\ell_1\ell_2\ell_3}$,

$$B_{m_1m_2m_3}^{\ell_1\ell_2\ell_3} = \mathcal{G}_{m_1m_2m_3}^{\ell_1\ell_2\ell_3} \times b_{\ell_1\ell_2\ell_3} , \quad (73)$$

where the Gaunt integral (of three $Y_{\ell m}$'s) is,

$$\mathcal{G}_{m_1m_2m_3}^{\ell_1\ell_2\ell_3} = \sqrt{\frac{(2\ell_1+1)(2\ell_2+1)(2\ell_3+1)}{4\pi}} \begin{pmatrix} \ell_1 & \ell_2 & \ell_3 \\ m_1 & m_2 & m_3 \end{pmatrix} \begin{pmatrix} \ell_1 & \ell_2 & \ell_3 \\ 0 & 0 & 0 \end{pmatrix} , \quad (74)$$

and the two parenthesized quantities are Wigner 3-j symbols. Also useful is the angle-averaged bi-spectrum,

$$B_{\ell_1\ell_2\ell_3} \equiv \sum_{m_1m_2m_3} \begin{pmatrix} \ell_1 & \ell_2 & \ell_3 \\ m_1 & m_2 & m_3 \end{pmatrix} \times B_{m_1m_2m_3}^{\ell_1\ell_2\ell_3} . \quad (75)$$

Each of the three correlators (72), (73) and (75) has an analogous observed quantity formed from the $a_{\ell m}^{\text{obs}}$'s. For example, the observed angle-averaged bi-spectrum is,

$$B_{\ell_1\ell_2\ell_3}^{\text{obs}} \equiv \sum_{m_1m_2m_3} \begin{pmatrix} \ell_1 & \ell_2 & \ell_3 \\ m_1 & m_2 & m_3 \end{pmatrix} \times a_{\ell_1m_1}^{\text{obs}} a_{\ell_2m_2}^{\text{obs}} a_{\ell_3m_3}^{\text{obs}} . \quad (76)$$

Given any one of the three correlators (72), (73) or (75), one can easily compute the other two. Expressions (73) and (75) define $b_{\ell_1\ell_2\ell_3}$ and $B_{\ell_1\ell_2\ell_3}$ in terms of $B_{m_1m_2m_3}^{\ell_1\ell_2\ell_3}$. Assuming the reduced angular bi-spectrum is known, one gets $B_{m_1m_2m_3}^{\ell_1\ell_2\ell_3}$ from (73) and $B_{\ell_1\ell_2\ell_3}$ from,

$$B_{\ell_1\ell_2\ell_3} = \sqrt{\frac{(2\ell_1+1)(2\ell_2+1)(2\ell_3+1)}{4\pi}} \begin{pmatrix} \ell_1 & \ell_2 & \ell_3 \\ 0 & 0 & 0 \end{pmatrix} \{\ell_1\ell_2\ell_3\} \times b_{\ell_1\ell_2\ell_3} , \quad (77)$$

where $\{\ell_1\ell_2\ell_3\}$ is the ‘‘triangular delta function’’ which vanishes unless $\ell_1 + \ell_2 + \ell_3$ even and $|\ell_i - \ell_j| \leq \ell_k \leq \ell_i + \ell_j$ for every different choice of i, j and k , in which case it gives one. The angle-averaged bi-spectrum implies,

$$B_{m_1m_2m_3}^{\ell_1\ell_2\ell_3} = \begin{pmatrix} \ell_1 & \ell_2 & \ell_3 \\ m_1 & m_2 & m_3 \end{pmatrix} \times B_{\ell_1\ell_2\ell_3} , \quad (78)$$

and inverting relation (77) gives $b_{\ell_1\ell_2\ell_3}$.

Just as expression (71) gives the C_ℓ 's in terms of the power spectrum (20), we would like a relation for the angular bi-spectrum in terms of its momentum-space cousin (21). Although this is well known, there are so many competing notational schemes that it is worth sketching the derivation. Substituting (69) in (72) and using (21) implies,

$$B_{m_1 m_2 m_3}^{\ell_1 \ell_2 \ell_3} = (4\pi)^3 (-i)^{\ell_1 + \ell_2 + \ell_3} \int \frac{d^3 k_1}{(2\pi)^3} \Delta_{\ell_1}(k_1) Y_{\ell_1 m_1}(\widehat{k}_1) \int \frac{d^3 k_2}{(2\pi)^3} \Delta_{\ell_2}(k_2) Y_{\ell_2 m_2}(\widehat{k}_2) \\ \times \int \frac{d^3 k_3}{(2\pi)^3} \Delta_{\ell_3}(k_3) Y_{\ell_3 m_3}(\widehat{k}_3) (2\pi)^3 \delta^3(\vec{k}_1 + \vec{k}_2 + \vec{k}_3) \times B(k_1, k_2, k_3) . \quad (79)$$

One now employs the identities,

$$(2\pi)^3 \delta^3(\vec{k}) = \int d^3 x e^{i\vec{k}\cdot\vec{x}} , \quad (80)$$

$$e^{i\vec{k}\cdot\vec{x}} = 4\pi \sum_{\ell=0}^{\infty} \sum_{m=-\ell}^{\ell} i^\ell Y_{\ell m}^*(\widehat{k}) Y_{\ell m}(\widehat{x}) j_\ell(kx) , \quad (81)$$

to reach the form,

$$B_{m_1 m_2 m_3}^{\ell_1 \ell_2 \ell_3} = \left(\frac{2}{\pi}\right)^3 \int_0^\infty dk_1 k_1^2 \Delta_{\ell_1}(k_1) \int_0^\infty dk_2 k_2^2 \Delta_{\ell_2}(k_2) \int_0^\infty dk_3 k_3^2 \Delta_{\ell_3}(k_3) \\ \times B(k_1, k_2, k_3) \times \int_0^\infty dx x^2 j_{\ell_1}(k_1 x) j_{\ell_2}(k_2 x) j_{\ell_3}(k_3 x) \times \mathcal{G}_{m_1 m_2 m_3}^{\ell_1 \ell_2 \ell_3} . \quad (82)$$

Comparison with expression (73) gives the reduced angular bi-spectrum,

$$b_{\ell_1 \ell_2 \ell_3} = \left(\frac{2}{\pi}\right)^3 \int_0^\infty dk_1 k_1^2 \Delta_{\ell_1}(k_1) \int_0^\infty dk_2 k_2^2 \Delta_{\ell_2}(k_2) \int_0^\infty dk_3 k_3^2 \Delta_{\ell_3}(k_3) \\ \times B(k_1, k_2, k_3) \times \int_0^\infty dx x^2 j_{\ell_1}(k_1 x) j_{\ell_2}(k_2 x) j_{\ell_3}(k_3 x) . \quad (83)$$

Wang and Kamionkowski worked out a recursive procedure for performing the integration over x on the second line of (83) [48]. We employed an improved technique devised by Mehrem [49]. The first feature occurs at the start of the first Doppler peak so it is roughly valid to make the Sachs-Wolfe approximation for the photon transfer functions,

$$\Delta_\ell(k) \longrightarrow \frac{1}{3} j_\ell(k\Delta\eta) , \quad (84)$$

where $\Delta\eta \simeq 0.956 \times H_0^{-1}$ is the conformal time from recombination to the present, expressed in terms of the current Hubble parameter. In order to avoid extensive numerical integration we approximated the spherical Bessel function and its square by delta functions,

$$j_\ell(z) \longrightarrow \frac{\delta(z-\ell)}{\sqrt{2\ell(\ell+1)}}, \quad (85)$$

$$j_\ell^2(z) \longrightarrow \frac{\delta(z-\ell)}{2\ell(\ell+1)}. \quad (86)$$

Using these approximations we computed the C_ℓ 's — from relation (71) — and the $B_{\ell_1\ell_2\ell_3}$'s — from relations (83) and (77) — in the range $10 \leq \ell \leq 50$ for the Square Well Model (65).

We are finally ready to discuss the problem of comparing a theoretical prediction for the angle-averaged bi-spectrum $B_{\ell_1\ell_2\ell_3}$ with the data $B_{\ell_1\ell_2\ell_3}^{\text{obs}}$. Babich has demonstrated the optimality of the estimator [47],

$$\mathcal{E} \equiv \frac{1}{\mathcal{N}^2} \sum_{\ell_1\ell_2\ell_3} \frac{\{\ell_1 \ell_2 \ell_3\} \times B_{\ell_1\ell_2\ell_3} \times B_{\ell_1\ell_2\ell_3}^{\text{obs}}}{C_{\ell_1} C_{\ell_2} C_{\ell_3}}. \quad (87)$$

The normalization factor \mathcal{N}^2 in expression (87) ensures that \mathcal{E} has unit mean,

$$\mathcal{N}^2 = \sum_{\ell_1\ell_2\ell_3} \frac{B_{\ell_1\ell_2\ell_3}^2}{C_{\ell_1} C_{\ell_2} C_{\ell_3}}. \quad (88)$$

We can estimate the variance of \mathcal{E} by assuming that the bi-spectrum is zero. To simplify the analysis, suppose z_i ($i = 1, \dots, N$) are independent, Gaussian random variables with mean zero and variance σ_i^2 . A symmetric \mathbf{C} -number constant q_{ijk} gives a cubic function of the z_i ,

$$Q \equiv \sum_{ijk=1}^N q_{ijk} z_i z_j z_k. \quad (89)$$

The mean of Q is zero and its variance is,

$$\sigma_Q^2 = \sum_{ijk=1}^N \sigma_i^2 \sigma_j^2 \sigma_k^2 \left[6q_{ijk}q_{ijk} + 9q_{iij}q_{kkj} \right]. \quad (90)$$

Making the appropriate substitution for the q_{ijk} gives,

$$\sigma_{\mathcal{E}}^2 = \frac{6}{\mathcal{N}^2} + \frac{9}{\mathcal{N}^4} \sum_{\ell_1 \ell_2 \ell_3} \frac{B_{\ell_1 \ell_1 \ell_2} B_{\ell_3 \ell_3 \ell_2}}{C_{\ell_1} C_{\ell_2} C_{\ell_3}} \times \sum_{m_1 m_2 m_3} \begin{pmatrix} \ell_1 & \ell_1 & \ell_2 \\ m_1 & m_1 & m_2 \end{pmatrix} \begin{pmatrix} \ell_3 & \ell_3 & \ell_2 \\ m_3 & m_3 & m_2 \end{pmatrix}. \quad (91)$$

The very similar analysis of Adshead, Dvorkin, Hu and Peiris reports the first term of expression (91) but not the second term [31].

The off-diagonal contribution to (90) seems to be a new effect so we took some trouble to understand both its sign and its magnitude. As long as the indices i , j and k are summed over the same index set the sign is positive,

$$\sum_{ijk=1}^N \sigma_i^2 \sigma_j^2 \sigma_k^2 q_{iij} q_{kkj} = \sum_{j=1}^N \sigma_j^2 \left(\sum_{i=1}^N \sigma_i^2 q_{iij} \right)^2. \quad (92)$$

We investigated whether it might be possible to get a negative result — which would *reduce* the total variance and *increase* the signal-to-noise ratio — by summing over carefully chosen, different index sets $i \in I$, $j \in J$ and $k \in K$. However, the Appendix proves that this cannot happen.

When one sums all indices over the same set the off-diagonal term tends to be suppressed because there are many combinations for which the diagonal contribution is nonzero but its off-diagonal cousin vanishes. Summing over the range $10 \leq \ell_i \leq 50$ results in the off-diagonal term being about a million times weaker than the diagonal contribution. However, its contribution can be significant when one sums over restricted index sets. Because this can never improve the signal-to-noise ratio we elected not to do it.

Our final result for a comparison between Planck data, using expression (76), and the predicted $B_{\ell_1 \ell_2 \ell_3}$ for the Square Well Model is,

$$\mathcal{E} = 0.36 \pm 196. \quad (93)$$

Although our estimate of the standard deviation is somewhat smaller than what Adshead, Hu, Dvorkin and Pereis found for a different model [31], we confirm their conclusion that the first feature “falls short of detectability by a very wide margin” [32].

6 Epilogue

We have examined the non-Gaussianity associated with conjectured sharp variations in the first slow roll parameter $\epsilon(n)$ known as “features”. In section 2 we identified the crucial contribution, equation (14), which becomes significant for features. Section 3 applied an approximation for how the scalar mode functions depend analytically on $\epsilon(n)$ [26, 34] to develop an approximation (30) for this term. Our result involves three tabulated functions of the instantaneous e-folding n and the e-folding of horizon crossing n_k :

1. $\tilde{g}(n, n_k)$ given in expression (33);
2. $\tilde{\gamma}'(n, n_k)$ given in expression (36); and
3. $\tilde{\phi}(n, n_k)$ given in expression (37).

Although generating these functions is numerically challenging, it only needs to be done over the narrow range of n and n_k associated with the feature. This is illustrated in Figure 3 which identifies the small ranges of n and n_k over which significant corrections would occur for a model of the first feature.

Our technique is more time-consuming, but also more accurate, than the approximation of Adshead, Dvorkin, Hu and Peiris [31]. Accuracy is important when studying features because they produce an oscillating signal, so even small errors in the phase can significantly degrade the signal. Figure 4 compares the two approximations for the equilateral triangle case of $k_1 = k_2 = k_3$. A numerical integration of the overlap indicates that employing the less accurate formula would sacrifice about one third of the signal.

In section 4 we presented a slight elaboration of a model due to Starobinsky [42] for which the crucial contribution (14) can be computed exactly, without any approximation [43–45]. In our model $\epsilon(n)$ jumps from ϵ_1 to ϵ_2 and then falls back down after an interval Δn , hence the name “Square Well Model”. Expression (56) gives the exact result for the bi-spectrum of the Square Well Model. However, taking the inessential factors of ϵ to zero produces a simpler and more transparent result (65) which is almost as accurate. A consequence of the sharp transitions is the persistence of oscillations for wave numbers which experience horizon crossing long after the transition. We regarded this as an artifact of the square well approximation, and truncated the late oscillations. For a different point of view we recommend the study of Adshead, Dvorkin, Hu and Lim [32].

In section 5 we transformed the momentum space bi-spectrum of theoretical considerations to the angular bi-spectrum which can be measured. We defined an estimator (87) for the first feature which represents an overlap between the theoretical prediction and observation. Note again the crucial importance of having an accurate theoretical prediction. Because the estimator is defined to have unit mean, the inverse of the square root of its variance gives the signal-to-noise ratio. Our result (91) for the variance seems to contain an extra, “off-diagonal” contribution in addition to the term found by Adshead, Dvorkin, Hu and Peiris [31]. Because the sign of this extra term seemed indefinite we investigated whether restricting the angular sums to non-symmetric regions might improve the signal-to-noise ratio. However, the Appendix proves that this can never happen. In the end, comparing the Square Wave Model with Planck data produced a null detection (93). We conclude that resolving the non-Gaussianity from a feature would require a signal about 200 times stronger.

A curious property of the variance (91) is that it seems to decrease as one includes more data, even for wave numbers long after the feature which are presumably unaffected by it. The apparent contradiction is resolved by noting that the theoretical prediction for the response of large wave numbers to a smooth, localized feature, tends to zero. However, one can see the obvious potential for noise to contaminate a real signal through the use of an inaccurate theoretical prediction.

Our study is somewhat different from the recent Planck analysis of theoretically motivated models for features [50] in that we employed no overarching model. What we did is better described as an attempt to cross-correlate power spectrum data with the angular bi-spectrum. However, our approximation (30) can be applied whenever $\epsilon(n)$ is known.

Acknowledgements

We are grateful to Jean-Luc Starck for assistance in accessing Planck data. This work was partially supported by the European Union’s Seventh Framework Programme (FP7-REGPOT-2012-2013-1) under grant agreement number 316165; by the European Union’s Horizon 2020 Programme under grant agreement 669288-SM-GRAV-ERC-2014-ADG; by NSF grants PHY-1506513 and 1806218; and by the UF’s Institute for Fundamental Theory.

7 Appendix: Varying the Index Sets

The purpose of this appendix is to prove that the second, “off-diagonal” contribution to the variance (90) is positive, even if the three (ℓ, m) pairs in the estimator are summed over different ranges. Hence the off-diagonal term can only degrade the signal-to-noise ratio, no matter what subset of data is analyzed. The quantity we wish to study is therefore,

$$Q \equiv \sum_{i \in I} \sum_{j \in J} \sum_{k \in K} q_{ijk} z_i z_j z_k, \quad (94)$$

where the \mathbf{C} -numbers q_{ijk} are symmetric with respect to all three indices but the index sets I, J and K are not necessarily the same.

Assuming the z_i 's are independent, Gaussian random variables with mean zero and variance σ_i^2 , the variance of Q is,

$$\langle Q^2 \rangle = \sum_{i \in I} \sum_{j \in J} \sum_{k \in K} q_{ijk} \sum_{\ell \in I} \sum_{m \in J} \sum_{n \in K} q_{lmn} \langle z_i z_j z_k z_\ell z_m z_n \rangle. \quad (95)$$

The expectation value of $z_i z_j z_k z_\ell z_m z_n$ gives 15 different terms, of which 6 are “diagonal” in the sense that each of the three indices in the second sum is paired with an index in the first sum, and 9 are “off-diagonal” in the sense that two of the indices of the first sum are paired and two of the indices of the second sum are paired.

Let us first consider the 6 diagonal pairings,

$$A_1 \equiv \sigma_i^2 \delta_{il} \times \sigma_j^2 \delta_{jm} \times \sigma_k^2 \delta_{kn}, \quad (96)$$

$$A_2 \equiv \sigma_i^2 \delta_{il} \times \sigma_j^2 \delta_{jn} \times \sigma_k^2 \delta_{km}, \quad (97)$$

$$A_3 \equiv \sigma_i^2 \delta_{im} \times \sigma_j^2 \delta_{jl} \times \sigma_k^2 \delta_{kn}, \quad (98)$$

$$A_4 \equiv \sigma_i^2 \delta_{im} \times \sigma_j^2 \delta_{jn} \times \sigma_k^2 \delta_{kl}, \quad (99)$$

$$A_5 \equiv \sigma_i^2 \delta_{in} \times \sigma_j^2 \delta_{jl} \times \sigma_k^2 \delta_{km}, \quad (100)$$

$$A_6 \equiv \sigma_i^2 \delta_{in} \times \sigma_j^2 \delta_{jm} \times \sigma_k^2 \delta_{kl}. \quad (101)$$

Because the q_{ijk} are totally symmetric, all six of these terms give sums over the same factors of $\sigma_i^2 \sigma_j^2 \sigma_k^2 (q_{ijk})^2$, but the ranges differ. The A_1 contribution gives the naive result,

$$A_1 \implies \sum_{i \in I} \sum_{j \in J} \sum_{k \in K} \sigma_i^2 \sigma_j^2 \sigma_k^2 (q_{ijk})^2. \quad (102)$$

However, the factor of δ_{jn} in A_2 can only contribute if $j \in J$ and also $j \in K$. In other words, j must belong to the intersection, $j \in J \cap K$. The same must be true for the index k so A_2 gives,

$$A_2 \implies \sum_{i \in I} \sum_{j \in J \cap K} \sum_{k \in J \cap K} \sigma_i^2 \sigma_j^2 \sigma_k^2 (q_{ijk})^2. \quad (103)$$

The four remaining diagonal pairings give,

$$A_3 \implies \sum_{i \in I \cap J} \sum_{j \in I \cap J} \sum_{k \in K} \sigma_i^2 \sigma_j^2 \sigma_k^2 (q_{ijk})^2, \quad (104)$$

$$A_4 \implies \sum_{i \in I \cap J} \sum_{j \in J \cap K} \sum_{k \in I \cap K} \sigma_i^2 \sigma_j^2 \sigma_k^2 (q_{ijk})^2, \quad (105)$$

$$A_5 \implies \sum_{i \in I \cap K} \sum_{j \in I \cap J} \sum_{k \in J \cap K} \sigma_i^2 \sigma_j^2 \sigma_k^2 (q_{ijk})^2, \quad (106)$$

$$A_6 \implies \sum_{i \in I \cap K} \sum_{j \in J} \sum_{k \in I \cap K} \sigma_i^2 \sigma_j^2 \sigma_k^2 (q_{ijk})^2. \quad (107)$$

Because the q_{ijk} are symmetric the contributions from A_4 and A_5 are the same, but the other contributions differ. They are each manifestly positive.

The 9 off-diagonal pairings are,

$$B_1 \equiv \sigma_i^2 \delta_{ij} \times \sigma_k^2 \delta_{kl} \times \sigma_m^2 \delta_{mn}, \quad (108)$$

$$B_2 \equiv \sigma_i^2 \delta_{ij} \times \sigma_k^2 \delta_{km} \times \sigma_\ell^2 \delta_{ln}, \quad (109)$$

$$B_3 \equiv \sigma_i^2 \delta_{ij} \times \sigma_k^2 \delta_{kn} \times \sigma_\ell^2 \delta_{lm}, \quad (110)$$

$$B_4 \equiv \sigma_i^2 \delta_{ik} \times \sigma_j^2 \delta_{jl} \times \sigma_m^2 \delta_{mn}, \quad (111)$$

$$B_5 \equiv \sigma_i^2 \delta_{ik} \times \sigma_j^2 \delta_{jm} \times \sigma_\ell^2 \delta_{ln}, \quad (112)$$

$$B_6 \equiv \sigma_i^2 \delta_{ik} \times \sigma_j^2 \delta_{jn} \times \sigma_\ell^2 \delta_{lm}, \quad (113)$$

$$B_7 \equiv \sigma_i^2 \delta_{il} \times \sigma_j^2 \delta_{jk} \times \sigma_m^2 \delta_{mn}, \quad (114)$$

$$B_8 \equiv \sigma_i^2 \delta_{im} \times \sigma_j^2 \delta_{jk} \times \sigma_\ell^2 \delta_{ln}, \quad (115)$$

$$B_9 \equiv \sigma_i^2 \delta_{in} \times \sigma_j^2 \delta_{jk} \times \sigma_\ell^2 \delta_{lm}. \quad (116)$$

By relabelling dummy indices and exploiting the symmetry of the q_{ijk} we can express each term as the same factor of $\sigma_i^2 \sigma_j^2 \sigma_k^2 q_{iik} q_{jjk}$ summed over different ranges. The results for each of the nine contributions are,

$$B_1 \implies \sum_{i \in I \cap J} \sum_{j \in J \cap K} \sum_{k \in I \cap K} \sigma_i^2 \sigma_j^2 \sigma_k^2 q_{iik} q_{jjk}, \quad (117)$$

$$B_2 \implies \sum_{i \in I \cap J} \sum_{j \in I \cap K} \sum_{k \in J \cap K} \sigma_i^2 \sigma_j^2 \sigma_k^2 q_{iik} q_{jjk} , \quad (118)$$

$$B_3 \implies \sum_{i \in I \cap J} \sum_{j \in I \cap J} \sum_{k \in K} \sigma_i^2 \sigma_j^2 \sigma_k^2 q_{iik} q_{jjk} , \quad (119)$$

$$B_4 \implies \sum_{i \in I \cap K} \sum_{j \in J \cap K} \sum_{k \in I \cap J} \sigma_i^2 \sigma_j^2 \sigma_k^2 q_{iik} q_{jjk} , \quad (120)$$

$$B_5 \implies \sum_{i \in I \cap K} \sum_{j \in I \cap K} \sum_{k \in J} \sigma_i^2 \sigma_j^2 \sigma_k^2 q_{iik} q_{jjk} , \quad (121)$$

$$B_6 \implies \sum_{i \in I \cap K} \sum_{j \in I \cap J} \sum_{k \in J \cap K} \sigma_i^2 \sigma_j^2 \sigma_k^2 q_{iik} q_{jjk} , \quad (122)$$

$$B_7 \implies \sum_{i \in J \cap K} \sum_{j \in J \cap K} \sum_{k \in I} \sigma_i^2 \sigma_j^2 \sigma_k^2 q_{iik} q_{jjk} , \quad (123)$$

$$B_8 \implies \sum_{i \in J \cap K} \sum_{j \in I \cap K} \sum_{k \in I \cap J} \sigma_i^2 \sigma_j^2 \sigma_k^2 q_{iik} q_{jjk} , \quad (124)$$

$$B_9 \implies \sum_{i \in J \cap K} \sum_{j \in I \cap J} \sum_{k \in I \cap K} \sigma_i^2 \sigma_j^2 \sigma_k^2 q_{iik} q_{jjk} . \quad (125)$$

Because the dummy indices i and j can be exchanged, B_1 gives the same as B_9 , B_2 gives the same as B_6 and B_4 gives the same as B_8 .

To obtain a manifestly positive form we decompose each set into parts which have no overlap. For example, the intersection between I and J can be decomposed into a part $\overline{I \cap J}$ which has not overlap with K , plus the intersection of all three sets. The analogous results for all three intersections are,

$$I \cap J = \overline{I \cap J} + I \cap J \cap K , \quad (126)$$

$$I \cap K = \overline{I \cap K} + I \cap J \cap K , \quad (127)$$

$$J \cap K = \overline{J \cap K} + I \cap J \cap K . \quad (128)$$

If we let \overline{I} stand for the part of I which has no overlap with either J or K then each of the three sets can be decomposed as,

$$I = \overline{I} + \overline{I \cap J} + \overline{I \cap K} + I \cap J \cap K , \quad (129)$$

$$J = \overline{J} + \overline{I \cap J} + \overline{J \cap K} + I \cap J \cap K , \quad (130)$$

$$K = \overline{K} + \overline{I \cap K} + \overline{J \cap K} + I \cap J \cap K . \quad (131)$$

To see how the decompositions (126-131) can be used consider the four B_i 's for which the index k is summed over the sets I , K and $I \cap K$,

$$B_3 = \sum_{k \in K} \sigma_k^2 \sum_{i \in I \cap J} \sigma_i^2 q_{iik} \sum_{j \in I \cap J} \sigma_j^2 q_{jjk}, \quad (132)$$

$$B_7 = \sum_{k \in I} \sigma_k^2 \sum_{i \in J \cap K} \sigma_i^2 q_{iik} \sum_{j \in J \cap K} \sigma_j^2 q_{jjk}, \quad (133)$$

$$B_1 + B_9 = 2 \sum_{k \in I \cap K} \sigma_k^2 \sum_{i \in I \cap J} \sigma_i^2 q_{iik} \sum_{j \in J \cap K} \sigma_j^2 q_{jjk}. \quad (134)$$

Now make the decompositions (129) in expression (132), (131) in expression (133, and (127) in (134). The parts involving $\overline{I \cap K}$ results in the positive form,

$$\sum_{k \in \overline{I \cap K}} \sigma_k^2 \left[\sum_{i \in I \cap J + J \cap K} \sigma_i^2 q_{iik} \right]^2. \quad (135)$$

Putting everything together gives a sum of positive terms,

$$\begin{aligned} \sum_{i=1}^9 B_i = & \sum_{k \in I \cap J \cap K} \sigma_k^2 \left[\sum_{i \in I \cap J + J \cap K + K \cap I} \sigma_i^2 q_{iik} \right]^2 + \sum_{k \in \overline{I \cap J}} \sigma_k^2 \left[\sum_{i \in I \cap K + J \cap K} \sigma_i^2 q_{iik} \right]^2 \\ & + \sum_{k \in \overline{J \cap K}} \sigma_k^2 \left[\sum_{i \in I \cap J + I \cap K} \sigma_i^2 q_{iik} \right]^2 + \sum_{k \in \overline{I \cap K}} \sigma_k^2 \left[\sum_{i \in I \cap J + J \cap K} \sigma_i^2 q_{iik} \right]^2 \\ & + \sum_{k \in \overline{I}} \sigma_k^2 \left[\sum_{i \in J \cap K} \sigma_i^2 q_{iik} \right]^2 + \sum_{k \in \overline{J}} \sigma_k^2 \left[\sum_{i \in I \cap K} \sigma_i^2 q_{iik} \right]^2 + \sum_{k \in \overline{K}} \sigma_k^2 \left[\sum_{i \in I \cap J} \sigma_i^2 q_{iik} \right]^2. \quad (136) \end{aligned}$$

References

- [1] V. F. Mukhanov and G. V. Chibisov, JETP Lett. **33**, 532 (1981) [Pisma Zh. Eksp. Teor. Fiz. **33**, 549 (1981)].
- [2] R. P. Woodard, Rept. Prog. Phys. **72**, 126002 (2009) doi:10.1088/0034-4885/72/12/126002 [arXiv:0907.4238 [gr-qc]].
- [3] A. Ashoorioon, P. S. Bhupal Dev and A. Mazumdar, Mod. Phys. Lett. A **29**, no. 30, 1450163 (2014) doi:10.1142/S0217732314501636 [arXiv:1211.4678 [hep-th]].

- [4] L. M. Krauss and F. Wilczek, Phys. Rev. D **89**, no. 4, 047501 (2014) doi:10.1103/PhysRevD.89.047501 [arXiv:1309.5343 [hep-th]].
- [5] N. Aghanim *et al.* [Planck Collaboration], arXiv:1807.06209 [astro-ph.CO].
- [6] P. A. R. Ade *et al.* [BICEP2 and Keck Array Collaborations], Phys. Rev. Lett. **116**, 031302 (2016) doi:10.1103/PhysRevLett.116.031302 [arXiv:1510.09217 [astro-ph.CO]].
- [7] N. C. Tsamis and R. P. Woodard, Annals Phys. **267**, 145 (1998) doi:10.1006/aphy.1998.5816 [hep-ph/9712331].
- [8] T. D. Saini, S. Raychaudhury, V. Sahni and A. A. Starobinsky, Phys. Rev. Lett. **85**, 1162 (2000) doi:10.1103/PhysRevLett.85.1162 [astro-ph/9910231].
- [9] T. Padmanabhan, Phys. Rev. D **66**, 021301 (2002) doi:10.1103/PhysRevD.66.021301 [hep-th/0204150].
- [10] S. Nojiri and S. D. Odintsov, Gen. Rel. Grav. **38**, 1285 (2006) doi:10.1007/s10714-006-0301-6 [hep-th/0506212].
- [11] R. P. Woodard, Lect. Notes Phys. **720**, 403 (2007) doi:10.1007/978-3-540-71013-4_14 [astro-ph/0601672].
- [12] Z. K. Guo, N. Ohta and Y. Z. Zhang, Mod. Phys. Lett. A **22**, 883 (2007) doi:10.1142/S0217732307022839 [astro-ph/0603109].
- [13] A. Ijjas, P. J. Steinhardt and A. Loeb, Phys. Lett. B **723**, 261 (2013) doi:10.1016/j.physletb.2013.05.023 [arXiv:1304.2785 [astro-ph.CO]].
- [14] A. H. Guth, D. I. Kaiser and Y. Nomura, Phys. Lett. B **733**, 112 (2014) doi:10.1016/j.physletb.2014.03.020 [arXiv:1312.7619 [astro-ph.CO]].
- [15] A. Linde, doi:10.1093/acprof:oso/9780198728856.003.0006 arXiv:1402.0526 [hep-th].
- [16] A. Ijjas, P. J. Steinhardt and A. Loeb, Phys. Lett. B **736**, 142 (2014) doi:10.1016/j.physletb.2014.07.012 [arXiv:1402.6980 [astro-ph.CO]].

- [17] P. A. R. Ade *et al.* [Planck Collaboration], *Astron. Astrophys.* **594**, A20 (2016) doi:10.1051/0004-6361/201525898 [arXiv:1502.02114 [astro-ph.CO]].
- [18] J. Torrado, B. Hu and A. Achucarro, *Phys. Rev. D* **96**, no. 8, 083515 (2017) doi:10.1103/PhysRevD.96.083515 [arXiv:1611.10350 [astro-ph.CO]].
- [19] J. Martin and C. Ringeval, *JCAP* **0608**, 009 (2006) doi:10.1088/1475-7516/2006/08/009 [astro-ph/0605367].
- [20] L. Covi, J. Hamann, A. Melchiorri, A. Slosar and I. Sorbera, *Phys. Rev. D* **74**, 083509 (2006) doi:10.1103/PhysRevD.74.083509 [astro-ph/0606452].
- [21] J. Hamann, L. Covi, A. Melchiorri and A. Slosar, *Phys. Rev. D* **76**, 023503 (2007) doi:10.1103/PhysRevD.76.023503 [astro-ph/0701380].
- [22] D. K. Hazra, A. Shafieloo, G. F. Smoot and A. A. Starobinsky, *JCAP* **1408** (2014) 048 doi:10.1088/1475-7516/2014/08/048 [arXiv:1405.2012 [astro-ph.CO]].
- [23] D. K. Hazra, A. Shafieloo, G. F. Smoot and A. A. Starobinsky, *JCAP* **1609**, no. 09, 009 (2016) doi:10.1088/1475-7516/2016/09/009 [arXiv:1605.02106 [astro-ph.CO]].
- [24] A. Achcarro, J. O. Gong, G. A. Palma and S. P. Patil, *Phys. Rev. D* **87**, no. 12, 121301 (2013) doi:10.1103/PhysRevD.87.121301 [arXiv:1211.5619 [astro-ph.CO]].
- [25] D. J. Brooker, N. C. Tsamis and R. P. Woodard, *Phys. Lett. B* **773**, 225 (2017) doi:10.1016/j.physletb.2017.08.027 [arXiv:1603.06399 [astro-ph.CO]].
- [26] D. J. Brooker, N. C. Tsamis and R. P. Woodard, *Phys. Rev. D* **96**, no. 10, 103531 (2017) doi:10.1103/PhysRevD.96.103531 [arXiv:1708.03253 [gr-qc]].
- [27] J. M. Maldacena, *JHEP* **0305**, 013 (2003) doi:10.1088/1126-6708/2003/05/013 [astro-ph/0210603].

- [28] J. R. Fergusson and E. P. S. Shellard, Phys. Rev. D **76**, 083523 (2007) doi:10.1103/PhysRevD.76.083523 [astro-ph/0612713].
- [29] J. R. Fergusson and E. P. S. Shellard, Phys. Rev. D **80**, 043510 (2009) doi:10.1103/PhysRevD.80.043510 [arXiv:0812.3413 [astro-ph]].
- [30] P. A. R. Ade *et al.* [Planck Collaboration], Astron. Astrophys. **594**, A17 (2016) doi:10.1051/0004-6361/201525836 [arXiv:1502.01592 [astro-ph.CO]].
- [31] P. Adshead, W. Hu, C. Dvorkin and H. V. Peiris, Phys. Rev. D **84**, 043519 (2011) doi:10.1103/PhysRevD.84.043519 [arXiv:1102.3435 [astro-ph.CO]].
- [32] P. Adshead, C. Dvorkin, W. Hu and E. A. Lim, Phys. Rev. D **85**, 023531 (2012) doi:10.1103/PhysRevD.85.023531 [arXiv:1110.3050 [astro-ph.CO]].
- [33] D. K. Hazra, L. Sriramkumar and J. Martin, JCAP **1305**, 026 (2013) doi:10.1088/1475-7516/2013/05/026 [arXiv:1201.0926 [astro-ph.CO]].
- [34] D. J. Brooker, N. C. Tsamis and R. P. Woodard, JCAP **1804**, no. 04, 003 (2018) doi:10.1088/1475-7516/2018/04/003 [arXiv:1712.03462 [gr-qc]].
- [35] A. R. Liddle, P. Parsons and J. D. Barrow, Phys. Rev. D **50**, 7222 (1994) doi:10.1103/PhysRevD.50.7222 [astro-ph/9408015].
- [36] V. F. Mukhanov, H. A. Feldman and R. H. Brandenberger, Phys. Rept. **215**, 203 (1992). doi:10.1016/0370-1573(92)90044-Z
- [37] A. R. Liddle and D. H. Lyth, Phys. Rept. **231**, 1 (1993) doi:10.1016/0370-1573(93)90114-S [astro-ph/9303019].
- [38] D. S. Salopek, J. R. Bond and J. M. Bardeen, Phys. Rev. D **40**, 1753 (1989). doi:10.1103/PhysRevD.40.1753
- [39] M. G. Romania, N. C. Tsamis and R. P. Woodard, JCAP **1208**, 029 (2012) doi:10.1088/1475-7516/2012/08/029 [arXiv:1207.3227 [astro-ph.CO]].
- [40] J. A. Adams, B. Cresswell and R. Easther, Phys. Rev. D **64**, 123514 (2001) doi:10.1103/PhysRevD.64.123514 [astro-ph/0102236].

- [41] M. J. Mortonson, C. Dvorkin, H. V. Peiris and W. Hu, Phys. Rev. D **79**, 103519 (2009) doi:10.1103/PhysRevD.79.103519 [arXiv:0903.4920 [astro-ph.CO]].
- [42] A. A. Starobinsky, JETP Lett. **55**, 489 (1992) [Pisma Zh. Eksp. Teor. Fiz. **55**, 477 (1992)].
- [43] F. Arroja, A. E. Romano and M. Sasaki, Phys. Rev. D **84**, 123503 (2011) doi:10.1103/PhysRevD.84.123503 [arXiv:1106.5384 [astro-ph.CO]].
- [44] J. Martin and L. Sriramkumar, JCAP **1201**, 008 (2012) doi:10.1088/1475-7516/2012/01/008 [arXiv:1109.5838 [astro-ph.CO]].
- [45] F. Arroja and M. Sasaki, JCAP **1208**, 012 (2012) doi:10.1088/1475-7516/2012/08/012 [arXiv:1204.6489 [astro-ph.CO]].
- [46] R. K. Sachs and A. M. Wolfe, Astrophys. J. **147**, 73 (1967) [Gen. Rel. Grav. **39**, 1929 (2007)]. doi:10.1007/s10714-007-0448-9
- [47] D. Babich, Phys. Rev. D **72**, 043003 (2005) doi:10.1103/PhysRevD.72.043003 [astro-ph/0503375].
- [48] L. M. Wang and M. Kamionkowski, Phys. Rev. D **61**, 063504 (2000) doi:10.1103/PhysRevD.61.063504 [astro-ph/9907431].
- [49] R. Mehrem, [arXiv:0909.0494 [math-ph]].
- [50] Y. Akrami *et al.* [Planck Collaboration], arXiv:1807.06211 [astro-ph.CO].